Article | Received 3 September 2025; Revised 30 September 2025; Accepted 23 October 2025; Published 30 October 2025
https://doi.org/10.55092/bm20250015

Chitosan nanoparticles for non-viral gene delivery: efficacy in immune cell transfection and *in vivo* studies

Mamatha Muraleedharan Pillai, Hemavathi Dhandapani, Manasa Srinivasan, Armaan Siddiqui and Prakriti Tayalia*

Department of Biosciences and Bioengineering, Indian Institute of Technology Bombay, Mumbai 400076, India

* Correspondence author; E-mail: prakriti@iitb.ac.in.

Highlights:

- Chitosan nanoparticles based non-viral gene delivery for immunotherapy applications.
- Efficient DNA transfection achieved in immune cells *in vitro*.
- Luciferase plasmid used to validate transfection efficiency *in vivo*.

Abstract: Immunotherapy represents an intervention in managing a wide variety of pathological diseases, including cancer and auto-immune disorders. The newest form of immunotherapy is cell and gene therapy, wherein immune cells are modified to express specific molecules and are genetically altered to generate a tailored immune response for a specific disease. While some of the viral vectors are FDA-approved and used as delivery vehicles, non-viral techniques are widely being explored for a safe and effective way to deliver genetic material to cells for therapeutic effect. Directed towards advancing a non-viral transfection system for immunotherapy, this study focuses on developing chitosan (CS) nanoparticles loaded with plasmid DNA (pDNA) and demonstrating their efficacy through both *in vitro* and *in vivo* transfection studies. These chitosan nanoparticles are synthesized via ionotropic gelation. When complexed with plasmid, they were found to be spherical in shape (~150 nm) and positively charged (zeta potential > 20 mV) as analyzed through dynamic light scattering (DLS), nanoparticle tracking analysis (NTA) and scanning electron microscopy (SEM). They exhibit good stability even after ten days of storage at 4 °C. Furthermore, their ability to transfect various immune cells *in vitro* was assessed using the GFP (green fluorescent protein) encoding plasmid. In addition, these nanoparticles loaded with luciferase (Luc) plasmid were assessed for their biodistribution and *in vivo* transfection in mice. Our results demonstrate that an optimized concentration of nanoparticles can be used for effective genetic modification of multiple immune cells *in vitro* as well as *in vivo*. Overall, these chitosan plasmid polyplexes hold promise as effective carriers of nucleic acid vaccines for immunotherapeutic applications.

Keywords: chitosan nanoparticles; transfection; T-cells; macrophages; immunotherapy; immune cells; *in vivo* transfection; biodistribution

1. Introduction

Immunotherapy has emerged as a revolutionary approach in the treatment of cancer and other immunological disorders, offering promising opportunities for personalized and targeted therapies. It involves the use of drugs, biologics, cell or gene modifying vectors to enhance or suppress the immune response and treat an immune-mediated disorder. Among various strategies employed in immunotherapy, immune cell gene engineering has received considerable attention because of the possibility of improving the effectiveness and selectivity of immunomodulatory therapies. This approach works on the mode of delivery of therapeutic genes into immune cells, which requires the creation of new generations of nanoparticles for gene delivery [1,2].

Commercial lipid-based gene delivery systems such as FuGene, GenePORTER, Transfast, DOTAP, and Lipofectamine 2000™ are positively charged and assist in encapsulating nucleic acids for cellular uptake through endocytosis. Lipofectamine 2000™ is broadly used for gene delivery, although toxicity restricts clinical use [3]. Cationic polymers such as poly(L-lysine) (PLL) on the other hand are characterized by poor endosomal escape and thus are less desirable for safe gene delivery. Polyethyleneimine (PEI) has been popular as an efficient non-viral gene delivery system, because it binds DNA over a broad pH range due to its wide range of buffering capacity. This helps in destabilizing endosomes by inducing an ion influx, thereby, releasing the genetic material into the cytoplasm. In spite of its high transfection efficiency, it has been found to exhibit considerable cytotoxicity, which restricts its clinical application [4]. These limitations coupled with the drawbacks of viral gene delivery systems such as increased immune and inflammatory responses, and limited cloning capacity necessitate the development of alternative non-viral gene delivery strategies. Some of the requirements for non-viral carriers include efficient cellular uptake, prevention of degradation of nucleic acids by enzymes, escape from endolysosomal compartments, efficient release of the genetic cargo, and nuclear entry into the cell. Scientists are synthesizing new polymers that are functionalized with CPPs (cell penetrating peptides), PEI or PF14 (similar to PEI) for gene delivery in immunotherapeutic applications [5]. However, from a translational perspective, there is a need to develop a non-toxic and stable transfection agent using natural polymers that can offer better biocompatibility.

Chitosan nanoparticles have been considered as promising non-viral vectors for gene delivery because of their inherent biocompatibility, biodegradability and immunomodulatory effects [1,2]. Their cationic nature enhances electrostatic interaction with the negatively charged nucleic acids for effective encapsulation and protection of therapeutic genes. Furthermore, chitosan nanoparticles have the ability to undergo endosomal escape which makes them suitable for cytosolic delivery of the genetic cargo [6]. Several studies have emphasized that the physical and chemical properties of chitosan–nucleic acid complexes determine efficient transfection, and a particle size of less than 500 nm and a positive surface charge are considered optimal for penetrating biological barriers. Such properties, and consequently the gene delivery efficacy, depend upon the type of chitosan and the process of formulation employed [7–9]. Chitosan's mucoadhesive property and its structural ability to undergo chemical modification makes it a versatile gene carrier. Chitosan nanoparticles have exhibited effective transfection *in vitro* in a variety of cell lines including HeLa, MG63, MSCs, CHO, U87, and HEK293 [8,10,11]. Even though chitosan nanoparticles have been well-explored for drug delivery applications, the potential of unmodified chitosan for immune cell engineering is less investigated. Lee *et al*. have reported that T-cell transfection

using siRNA-loaded chitosan nanoparticles, modified using carbodiimide-mediated conjugation for CD4+ T-cell specificity has shown promising results [12]. While the *in vitro* results were encouraging, the *in vivo* efficacy of these modified nanoparticles remains to be assessed and optimized.

In this study, we synthesized chitosan nanoparticles encapsulating GFP plasmid and conducted *in vitro* transfection experiments in T-cells and macrophages, which are two important components of the immune system. By investigating gene delivery in different immune cell types, this study aims to shed light on the versatility and efficacy of chitosan nanoparticles in enhancing immunotherapy for various immunological disorders. Additionally, demonstration of these nanoparticles for effective *in vivo* gene delivery in mice suggests their potential for translational applications.

2. Methods

2.1. Plasmid isolation and purification

In this study, two plasmids, namely, pGFP (encoding green fluorescence protein) and pLuc (encoding both luciferase and red fluorescent protein), were used for *in vitro* and *in vivo* studies, respectively. To propagate these plasmids, Escherichia coli bacterial strains were cultured on Luria-Bertani (LB) agar plates containing 100 µg/mL ampicillin and incubated overnight at 37 °C. Selected colonies were then transferred to a one-liter flask with LB medium, supplemented with ampicillin. Cultures were grown on a shaker incubator at 37 °C, 250 rpm until the optical density (OD) reached 2.6, indicating exponential growth. The cultures were scaled up by transferring to larger Erlenmeyer flasks containing LB medium and incubated overnight. Bacterial cells were harvested by centrifugation and stored at −20 °C. The plasmid (pDNA) was extracted and purified using the Nucleobond Xtra Midi EF kit (Macherey-Nagel, US) according to the manufacturer's instructions. The concentration of purified pDNA was measured using a Nanodrop system (Multimode Microplate Reader Varioskan LUX, ThermoScientific).

2.2. Preparation of nanoparticles

The chitosan (CS) nanoparticles were prepared using ionotropic gelation with chitosan as the polymer and tripolyphosphate (TPP) as the crosslinker. CS (medium molecular weight and 75%–85% deacetylated) and TPP were obtained from Merck. Chitosan solution (0.25% or 0.5% w/v) was prepared in 1% (v/v) acetic acid, and TPP stock solution (0.125%, 0.25% or 0.35% w/v) was prepared in deionized water. Both solutions were filtered through a 0.2 µm polyethersulfone syringe filter. These nanoparticles were prepared either with or without addition of NaCl (150 mM).

300 µg of pDNA (pGFP or pLuc) was dissolved in 10 mL of TPP solution. Using a syringe pump, the TPP or TPP-pDNA solutions were added dropwise to the CS solution at the rate of 0.5 mL/min using a 20 G needle while the solution was being stirred at a speed of 600 rpm on a magnetic stirrer. After the addition was complete, the mixture was stirred for an additional 30 minutes and centrifuged at 10,000 rpm for 10 minutes at 4 °C. After the removal of supernatant, the pellet was resuspended in phosphate buffered saline (PBS), frozen at −80 °C overnight and lyophilized for 24 hours. For all subsequent experiments, the lyophilized powder was dissolved in 2 ml of sterile deionized water and stored at 4 °C. CS nanoparticles crosslinked with TPP and complexed with or without plasmid DNA are referred to as CSNP or pCSNP, respectively.

2.3. Characterization of nanoparticles

2.3.1. Particle size analysis

The size and charge of CSNP and pCSNP were analyzed through Dynamic Light Scattering (DLS) using the Zetasizer Nano ZS analyzer (Malvern Instruments, UK). Stability of the nanoparticles was assessed by studying their aggregation using DLS and Zetasizer software. Measurements were taken immediately after preparation, then 72 hours and 10 days after being stored at 4 °C in deionised water. The size distribution was also analyzed using nanoparticle tracking analysis (NTA) NanoSight NS300 (Malvern Instruments, UK). The morphology of both CSNP and pCSNP was examined using scanning electron microscope (SEM, FEI Quanta 200) and transmission electron microscope (TEM, Themis 300 G3, Thermo). For this, the freshly prepared nanoparticles (CSNP and pCSNP) were centrifuged (10,000 rpm, 10 min, 4 °C) and the supernatant was discarded. The pellet was resuspended in phosphate-buffered saline (PBS) solution, centrifuged again, resuspended in deionized water and sonicated for 5 minutes. Samples were loaded on aluminum stubs, air dried and sputtered with gold to perform SEM. Samples were loaded onto a copper grid for TEM imaging and dried overnight at room temperature.

2.3.2. pDNA encapsulation estimation

To assess the amount of pDNA encapsulated in the nanoparticles, the NPs were centrifuged for 10 minutes at 10,000 rpm subsequent to the stirring step in the synthesis process. The concentration of DNA in the supernatant was measured at 260 nm. The encapsulation efficiency (EE) was calculated using the following formula:

$$EE = ((C_{total} - C_{suspension})/C_{total}) \times 100$$

where C_{total} is the initial pDNA concentration in the solution; $C_{suspension}$ is the pDNA concentration in the supernatant after the encapsulation process.

2.3.3. Gel retardation for binding of pDNA to nanoparticles

Gel retardation analysis was performed to assess the stability of pDNA incorporation into the chitosan nanoparticles. For this, 1% agarose gel was prepared by dissolving 0.4 g of agarose in 40 mL of TAE 1 × buffer (40 mM Tris base, 20 mM acetic acid, 1 mM EDTA at pH 8.0) with 1 µL of ethidium bromide. 18 µL of each sample (such as ladder, pDNA, CSNP and pCSNP) along with 2 µL of loading buffer were loaded into the wells. Electrophoresis was done at 120 V for 40 minutes, and the gel was analyzed using the Chemidoc imaging system (Bio-rad).

2.4. In vitro cytocompatibility analysis

Mouse NIH-3T3 fibroblasts and Lenti-X cells were used to test the cytocompatibility of the pCSNP (with Luc plasmid). Briefly, 0.70 lakh cells/well of NIH-3T3 and 0.5 lakh cells/well of Lenti-X were seeded in a 12-well plate and incubated overnight at 37 °C in a CO_2 incubator. The resuspended pCSNP were added in volumes ranging from 20 µL to 80 µL to the cells such that the concentration of plasmid

varied from 3 µg to 12 µg. After 48 hrs, the cell proliferation in control and pCSNP treated conditions was assessed using MTT (3-(4,5-dimethylthiazol-2-yl)-2,5-diphenyltetrazolium bromide) assay (Himedia). Briefly, media in the wells was removed, 500 µL of MTT (5 mg/ml) was added to each well and incubated for 4 hrs. After this, MTT was removed and 500 µL DMSO (dimethyl sulfoxide, Himedia) was added to the wells to dissolve the formazan crystals and incubated for 30 minutes with gentle rocking. Absorbance of the resulting homogeneous solution was measured at 570 nm using a spectrophotometer.

2.5. Cell transfection analysis

In vitro transfection was performed in different cells, including Lenti-X, Jurkat T-cells, THP-1, THP-1 derived macrophages and splenocytes. Splenocytes were isolated from C57BL/6 mice as per the protocol approved by the Institute Animal Ethics Committee (IAEC 01/2022). For THP-1 derived macrophages, THP-1 cells were seeded at 2 lakh cells/well in 24-well plates followed by addition of 10 ng/ml of PMA (phorbol 12-myristate 13-acetate) and incubated for 48 hrs. The adherent THP-1 derived macrophage cells were used further for transfection. The lyophilized pCSNP nanoparticles carrying GFP plasmid were suspended in 2 ml of sterile deionized water and added to Lenti-X cells in volumes ranging from 10 µl to 80 µl, such that the plasmid concentration varied between 1.5 µg to 12 µg. PEI was used as another transfection agent and a positive control with 3 µg of plasmid at a 1:3 ratio of PEI:DNA. The optimized concentration of pCSNP was used for all other cells in this study. Briefly, 1 lakh cells/well were seeded in a 12-well plate and incubated overnight at 37 °C in a 5% CO2 incubator. After overnight incubation, 40 µl of nanoparticles containing 6 µg of GFP plasmid was added dropwise to the cells. After 72 hours of incubation, adherent cells such as Lenti-X and macrophages were detached from the culture plate using a scraper and collected in 1.5 ml centrifuge tubes. Non-adherent cells such as Jurkat T-cells, THP-1, and splenocytes were directly collected in 1.5 ml centrifuge tubes. These cells were centrifuged at 1500 rpm for 5 minutes, washed once with PBS, and resuspended in 300 µl of PBS. Splenocytes were further stained with anti-CD3 PE (BioLegend, US) and anti-CD11c APC (Invitrogen, US) for 20 minutes at room temperature. After incubation, the cells were washed and suspended in 300 µl of PBS and analyzed using a flow cytometer (FACS Aria, BD Biosciences, USA) with excitation at 488 nm and emission at 525 nm or 530 nm for detecting GFP or Luc expression, respectively. For Lenti-X, Jurkat T-cells, THP-1 cells and THP-1 derived macrophages, the respective untreated cells were used for gating to set the baseline GFP fluorescence. For splenocytes, within the CD3+ or CD11c+ gated cells, the untreated cells were used for gating. FlowJo v9.0 software was used for all subsequent analysis of the acquired data.

2.6. In vivo experiments

All animal experiments were conducted at the Laboratory Animal Facility, Advanced Centre for Treatment, Research and Education in Cancer (ACTREC), Mumbai as per the protocols approved by the Institute Animal Ethics Committee (IAEC 01/2022).

2.6.1. *In vivo* biocompatibility and biodistribution study

The *in vivo* biocompatibility of CSNPs was evaluated in BALB/c mice. To prepare the nanoparticle solution, 0.25% chitosan and 0.35% TPP (with or without 300 µg of pLuc) and 150 mM NaCl were used,

following the procedure described in Section 2.2. The particles were then lyophilized and reconstituted in 2 mL of sterile deionized water for injection. Six animals per group were used, CSNPs were administered intraperitoneally at two different doses: 200 µL (LD) and 400 µL (HD). After 48 hours, spleens were harvested from mice, and single-cell suspensions were prepared by mechanical disruption and red-blood cell lysis. The cells were stained with anti-CD3 PB (Invitrogen, USA) anti-CD4 APC (Invitrogen, USA), anti-CD8 PE (Invitrogen, USA), anti-CD86 PE (Invitrogen, USA), anti-CD14 PE (Invitrogen, USA), and anti-CD69 PE (BD Biosciences, USA) and incubated at room temperature for 20 minutes. The cells were subsequently washed and suspended in 300 µl of PBS and analyzed using a flow cytometer (Cytoflex, Beckmann Coulter).

Nanoparticles containing indocyanine green (ICG) or Aurogreen (25 mg), which is an IR780 dye, were prepared to investigate biodistribution in BALB/c mice. Briefly, 0.5 mg/ml of ICG was added to the CS solution and TPP was added for the preparation of nanoparticles (CSNP-ICG). Excess dye was removed by washing and centrifuging the solution three times. Three groups, each consisting of four mice, were included in the study: untreated, those injected with ICG alone and those injected with CSNP-ICG.

200 µL of the nanoparticle solution was injected via tail vein in BALB/c mice, which were immediately imaged live using an IVIS Lumina II imaging system (PerkinElmer, Waltham, MA, USA). Subsequently, the animals were euthanized, and organs were collected for imaging again using the IVIS system with the following settings: excitation filter: 745 nm, emission filter: ICG, exposure time: 2 s, binning factor: medium, f/Stop: 2, field of view: D. Quantitative analysis of fluorescence was performed using Living Image Software 4.3.1 (Perkin Elmer, Waltham, MA, USA) along with the Image Math tool. This facilitated the subtraction of the background tissue autofluorescence from the ICG signal, ensuring accurate image processing and quantification.

2.6.2. *In vivo* transfection analysis

To analyze *in vivo* transfection, pCSNP-Luc nanoparticles were used and luciferase expression was monitored using the IVIS imaging system. Briefly, 7-week-old BALB/c mice were used in groups of four and injected intraperitoneally with 200 µL of CS nanoparticles, with (30 µg of pLuc plasmid) or without luciferase plasmid, using insulin syringes with 28G needles. After 48 hours, animals were imaged live using IVIS, after which organs were explanted and imaged again for transfection analysis. The animals were placed in a lightproof chamber, and bioluminescence images were acquired for a total of five minutes until the peak emission was confirmed. Bioluminescence signal indicated the luciferase expression from cells transfected by pCSNP-Luc nanoparticles. Grayscale and bioluminescence images were overlaid using imaging software (PerkinElmer).

2.7. Statistical analysis

Experiments were conducted in triplicates (n = 3). Results are presented as mean ± standard deviation (S.D.). Statistical analyses were performed using one-way analysis of variance (ANOVA). Data were analyzed with GraphPad Prism 6 software, and a p-value of less than 0.05 was considered as statistically significant.

3. Results and discussions

The synthesis of CSNP particles was optimized by varying the concentrations of chitosan (CS) and tripolyphosphate (TPP), with and without NaCl. The criterion of optimization was to obtain stable nanoparticles with uniform size distribution (Table 1). Using 0.25% CS and 0.35% TPP resulted in nanoparticles with reproducible size and stability, consistently measuring below 200 nm. The amines in the cationic chitosan crosslink with the pentavalent TPP anions. Factors affecting the size and stability of particles include the ratio of chitosan and TPP, which changes the crosslinking of chitosan and subsequently, its ability to swell and aggregate. Monovalent ions from the salt can enhance the binding strength between CS and TPP by competitively binding with multivalent ions, resulting in less aggregation and smaller-sized particles [13]. As shown in Table 1, it was evident that more stable and smaller particles can be achieved by using NaCl. The GFP plasmid was incorporated into the CSNP resulting in pCSNP with a plasmid encapsulation efficiency of 86%.

Table 1. Optimization of CSNP size.

Chitosan (w/v %)	TPP (w/v %)	NaCl (mM)	Z average (nm)	Size (nm)	Polydispersity Index (PDI)	Inference
0.25	0.125	-	1079	543.1 ± 115	1	Faster aggregation. Less concentration of TPP may not be sufficient to crosslink
0.5	0.125	-	5881	Varying range	1	Unstable particles
0.25	0.25	-	1520	890 ± 132.6	0.48	Large particles, settling may cause instability
0.5	0.25	-	1960	892.1 ± 113.6	0.44	Large particles, settling may cause instability
0.5	0.35	-	2927	256.4 ± 26.6	1	Large particles, settling may cause instability
0.5	0.5	-	1594	453 ± 51.4	1	Z average is high, could lead to low particle stability
0.25	0.25	1 ml	1.5×10^4	Not detectable	-	Large size
0.5	0.25	1 ml	6801	398.2 ± 41.3	1	Stable particles
0.25	0.35	1 ml	8380	101.8 ± 12.5	0.06	Stable particles

3.1. CSNP nanoparticle size and stability studies

The size of pCSNP was examined using various techniques such as SEM, TEM and DLS. SEM images, as shown in Figure 1a,d, reveal that the formulated NPs exhibit a spherical shape and uniform morphology. The size of the nanoparticles was measured using ImageJ software, with the size distribution shown in Figure 1b,e. The sizes of CSNP and pCSNP were 102.9 ± 43.9 nm and 119.1 ± 34.2 nm, respectively. The hydrodynamic radius of the nanoparticles was analyzed using DLS, showing sizes of 100.4 ± 30.8 nm

and 152.3 ± 56.2 nm for CSNP and pCSNP, respectively (Figure 1c,f). The size distribution obtained from NTA analyses also indicates that the majority of nanoparticles were below 200 nm for both CSNP and pCSNP (Figure S1a,b). TEM images of CSNP and pCSNP show a particle size of 175.9 ± 30.5 nm and 169.6 ± 37 nm, respectively (Figure 1g,h). The zeta potential was also found to be ideal, at +21.02 mV and +16.2 mV for CSNP and pCSNP, respectively (Figure 1i,j). Addition of plasmid reduces the zeta potential of CSNP due to the negative charge of DNA. Gel retardation assay was performed using electrophoresis to evaluate the stability and complexation of DNA with chitosan in pCSNP (Figure 1k). It was observed that pDNA migrates faster when loaded alone (in second lane) while pCSNP (in fourth lane) stays in the well itself, demonstrating that the chitosan-DNA polyplex does not allow the pDNA to migrate, thereby, confirming the stability of pCSNP nanoparticles. These results are in line with other studies with CSNP nanoparticles, where the crosslinker TPP plays a significant role in stabilizing the particles [14–17]. The size of the nanoparticles should ideally be below 200 nm to allow strong cellular uptake by endocytosis [18]. It has been demonstrated by various researchers that NPs with spherical morphology exhibit significantly greater cellular internalization compared to rod-shaped NPs [15]. Surface charge of the nanoparticles also affects the stability of nanoparticles and cellular uptake. Positively charged nanoparticles are capable of binding to the anionic cell membrane and molecular motor proteins in order to move towards the cell nucleus for gene transfer [16,17]. In view of these reports, the nanoparticles prepared in this study were also found to exhibit ideal size, morphology and surface charge for cellular uptake.

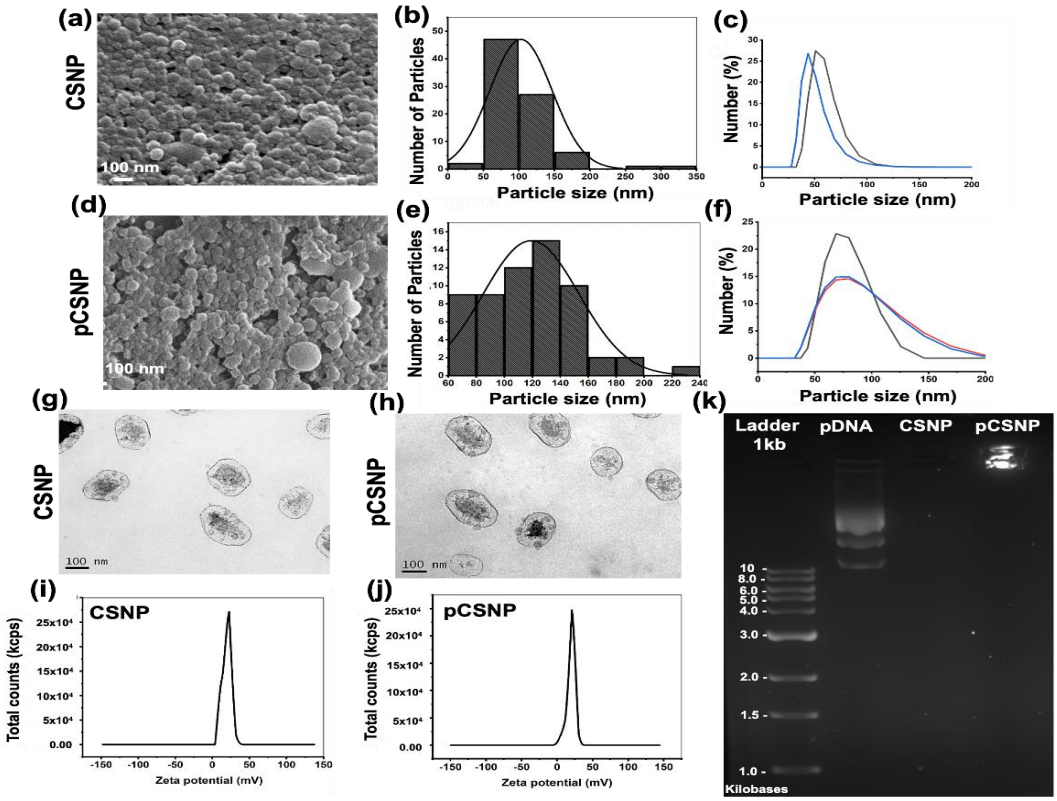

Figure 1. Characterization of CSNP and pCSNP. **(a)** SEM images of CSNP and their size distribution obtained from **(b)** SEM, **(c)** DLS. **(d)** SEM images of pCSNP and their size distribution obtained from **(e)** SEM, **(f)** DLS. TEM images of **(g)** CSNP and **(h)** pCSNP. Zeta potential of **(i)** CSNP and **(j)** pCSNP. **(k)** Gel retardation assay showing complexation of plasmid with CSNP.

3.2. In vitro cytocompatibility and transfection of immune cells

The cytocompatibility of the pCSNP-Luc was evaluated using MTT metabolic activity assay over a range of plasmid concentrations. It was observed that the concentrations tested were not cytotoxic to the NIH-3T3 and Lenti-X cells (Figure S2a,b, respectively). Again, the concentration of pCSNP for optimal transfection was found by varying the quantities of pCSNP-GFP added to Lenti-X cells (Figure S3). The positive control used here was PEI, which is a cationic polymer, known to be very effective in transfecting adherent cell lines owing to its excellent DNA compaction ability and intrinsic endosomolytic activity [4]. Using the gating strategy defined earlier, the GFP+ cells were identified to determine the transfection efficiency. It was observed that 40 µl of pCSNP containing 6 µg of plasmid significantly increased the percentage of transfected cells (69.3% ± 2.3%) when compared to other concentrations (Figure S3). Subsequently, the same concentration was used to transfect other immune cells, including human T-cell line (Jurkat), human monocyte cell line (THP-1), and THP-1 derived macrophages, which showed a transfection efficiency of 19.7% ± 6.3%, 19.0% ± 5.4% and 29.4% ± 15.3%, respectively (Figure 2a–c). Splenocytes isolated from C57BL/6 mice were also transfected and the cells gated for GFP+ in the CD3+ and CD11c+ subsets were found to be 17.1% ± 0.5% and 12.4% ± 0.7%, respectively (Figure 2d).

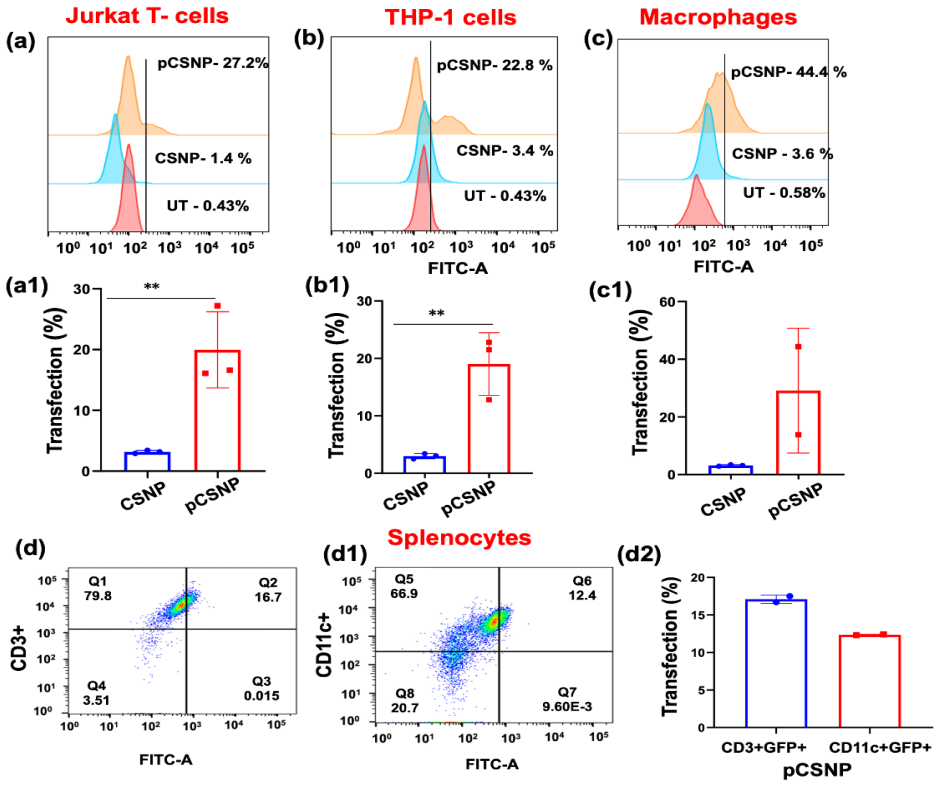

Figure 2. *In vitro* immune cell transfection efficiency of chitosan nanoparticles. Flow cytometry analysis shown using **(a–c)** Representative histograms and **(a1–c1)** Bar graphs showing the quantification of transfected cell population with optimized concentration of pCSNPs in Jurkat T-cells, THP-1 cells and THP-1 derived macrophages, respectively (n = 3, mean ± s.d.) (UT: untreated cells). Flow cytometry dot plot representation of pCSNP transfected splenocytes showing **(d)** CD3+ and **(d1)** CD11+ cells, and their corresponding **(d2)** Bar graph quantification showing transfection percentage.

While chitosan nanoparticles have been extensively explored for gene delivery in the adherent epithelial or cancer cells, their potential to transfect immune cells such as T cells, monocytes and primary splenocytes is not well-reported. Further, non-viral gene delivery is quite challenging in T-cells, thereby, limiting their immunotherapeutic applications [19]. Typically, lentiviral vectors or nucleofection has been reported for gene modulation in splenocytes. In this study, however, pCSNP showed good transfection in both Jurkat T-cells as well as splenocytes. The mechanism of CSNP uptake has been described by many researchers as an endocytic transport mechanism of charged biomolecules across the cell membrane [18,20,21]. The results in this study demonstrate the consistent transfection efficacy of the developed chitosan nanoparticles across different immune cell types enabled by efficient cellular internalization and subsequent gene expression.

3.3. In vivo biocompatibility analysis

The effect of systemic administration of chitosan nanoparticles was assessed by profiling the splenocytes harvested from the treated mice. As compared to the control (untreated) mice, there was no significant difference in the percentage of cells positive for various T-cell markers including CD3, CD4, CD8 and CD69 in the treated mice, indicating that CSNP administration did not impact the numbers and activation status of the splenic T-cells (Figure 3a–d). In addition, the expression of CD14, a marker for monocytes, was also comparable between the control and the treated groups (Figure 3f).

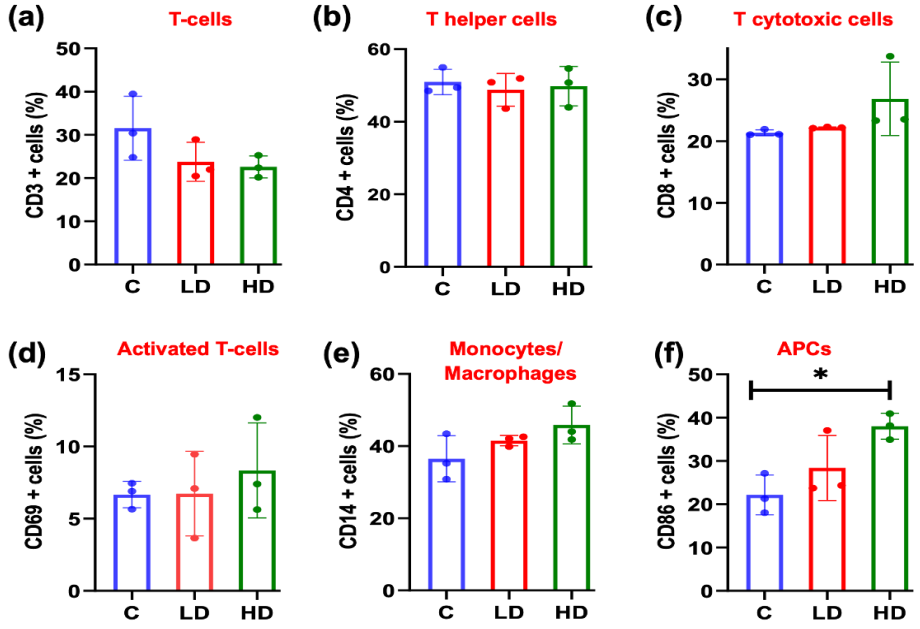

Figure 3. Flow cytometry analysis showing *in vivo* immunocompatibility of CSNP, evaluated by subjecting mice to varying doses of CSNPs and looking at the effect on their splenocytes, depicted by various immune cell specific surface markers, namely, **(a)** CD3 (T-cells), **(b)** CD4 (T helper cells), **(c)** CD8 (cytotoxic T-cells), **(d)** CD69 (activated T-cells), **(e)** CD14 (monocytes and macrophages) and **(f)** CD86 (antigen presenting cells), when treated with PBS control (C), low dose (LD-200 µL) and high dose (HD-400 µL) of CSNPs. Statistical analysis was performed using a one-way ANOVA test. (n = 3 mice per group; * $p < 0.05$).

However, treatment with higher dose of CSNP resulted in a slightly increased expression of CD86, a co-stimulatory molecule on the surface of antigen presenting cells including dendritic cells, macrophages and B cells (Figure 3e). The above analysis suggested that CSNPs do not elicit a noticeable immune response at low doses, thereby validating their biocompatibility for *in vivo* studies. Hence, a concentration of 200 µL of CSNPs was used for subsequent *in vivo* transfection studies.

3.4. In vivo biodistribution and transfection analysis

CSNP-ICG nanoparticles were injected via the tail vein in BALB/C mice as shown in the schematic in Figure 4a. Biodistribution analysis revealed a strong signal throughout the body within 10 minutes of injection, demonstrating widespread distribution of CSNP-ICG in mice (Figure 4b). Subsequently, various organs such as liver, spleen, kidneys and heart were explanted and also showed a strong signal due to the presence of ICG dye or CSNP-ICG nanoparticles (Figure 4c,d). Figure 4e depicts the quantification of average radiant efficiency from explanted organs showing the strongest signal in the liver followed by lungs, kidneys, spleen and heart. This indicates that the biodistribution of CSNPs is based on uptake by the reticuloendothelial system (RES) as also reported previously [6].

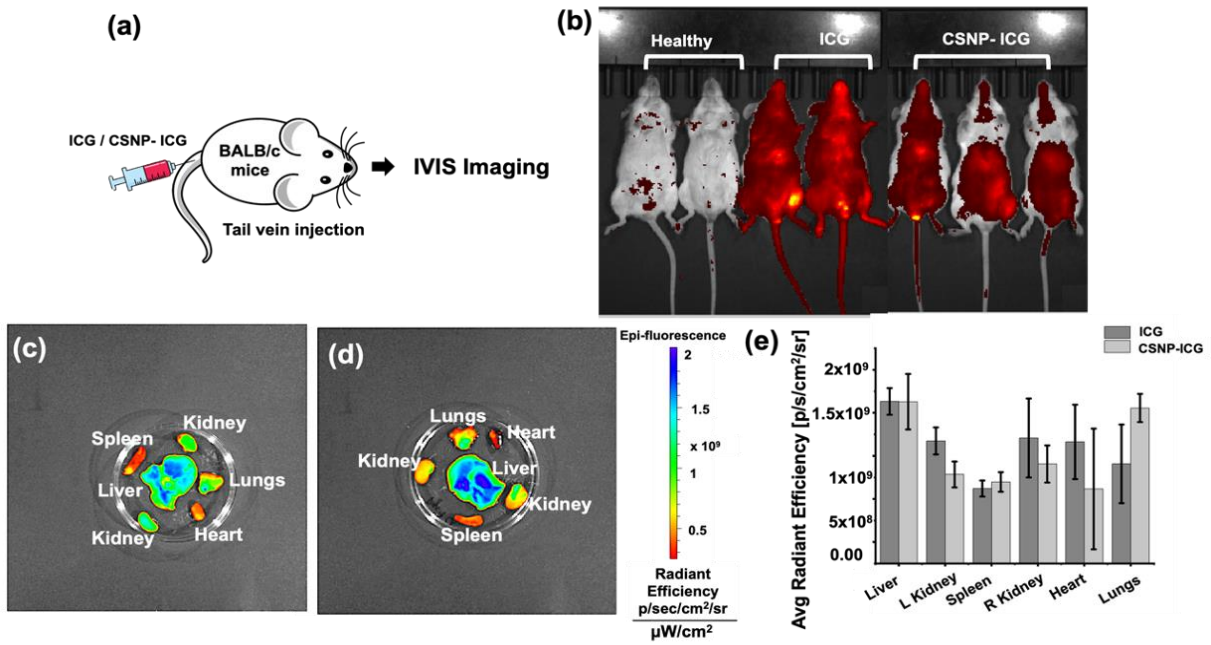

Figure 4. Biodistribution of CSNP in Balb/c mice **(a)** Schematic showing injection of ICG or CSNP-ICG in mice. **(b)** IVIS image showing *in vivo* bioluminescence in live mice when injected with ICG only or CSNP-ICG nanoparticles. *Ex vivo* bioluminescence in explanted organs comparing injection of **(c)** ICG only and **(d)** CSNP-ICG nanoparticles. **(e)** Quantification of average radiant efficiency from each organ for both conditions. (n = 4 mice per group)

To assess *in vivo* transfection efficiency, 200 µL of pCSNP-Luc was injected intraperitoneally as shown in the schematic (Figure 5a). After 48 hours, strong signals of bioluminescence were observed in the abdominal region of pCSNP-Luc treated mice in contrast to those injected with CSNP without plasmid, where no signal was observed (Figure 5b,c). This suggests that more uptake and subsequent transfection was taking place in the liver and spleen. The explanted organs also showed similar results,

confirming the successful delivery and expression of the plasmid, pLuc delivered via chitosan nanoparticles (CSNPs) (Figure 5d,e). Figure 5f depicts the quantification of bioluminescence from the region of interest (ROI) in mice which exhibited a strong signal from pCSNP compared to CSNP. The mechanism of chitosan transfection may involve several key steps, including uptake by the cells through endocytosis and subsequent escape from the endosomes to release the pDNA cargo into the cytoplasm. This escape is facilitated by the interaction between chitosan and anionic lipids of the endosomal membrane, leading to the disruption of the membrane, followed by the release of DNA into the cytoplasm [22]. However, further studies need to be conducted to elucidate the precise mechanism of CSNP-mediated gene delivery demonstrated here.

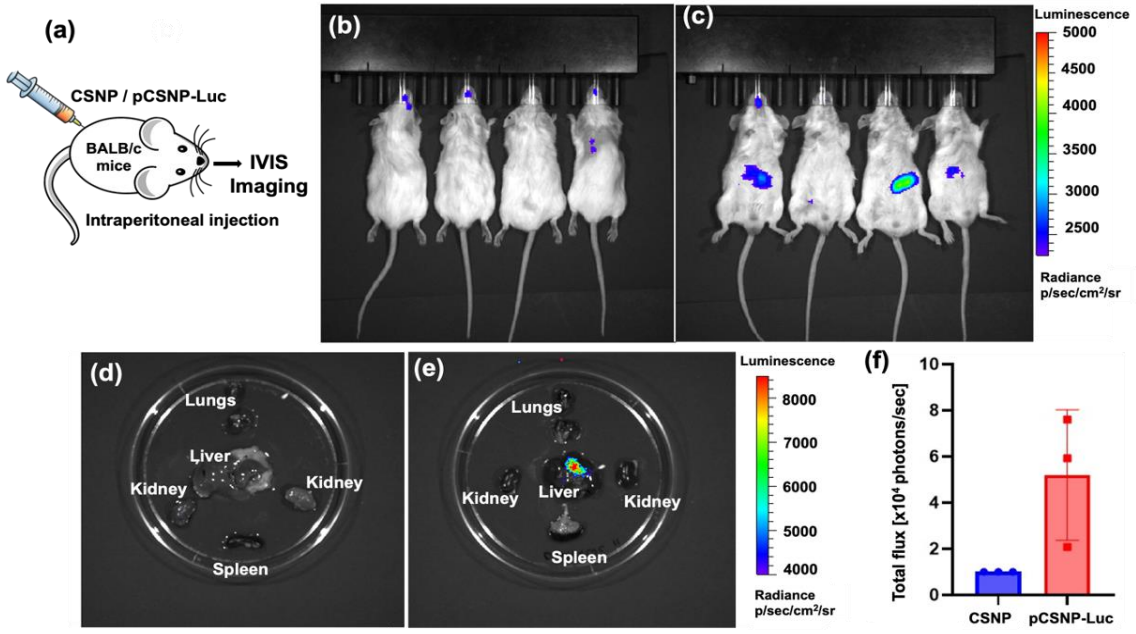

Figure 5. *In vivo* transfection efficiency of CSNP **(a)** Schematic showing injection of CSNP or pCSNP-Luc in Balb/c mice. **(b)** IVIS image showing *in vivo* bioluminescence in live mice when injected with **(b)** CSNP or **(c)** pCSNP-Luc. *Ex vivo* bioluminescence in explanted organs measured 48 hours after injection of **(d)** CSNP or **(e)** pCSNP-Luc. **(f)** Quantification of bioluminescence in live mice for both conditions.

This study showcases the potential of the developed pCSNPs for successful *in vivo* transfection. However, to effectively transfect immune cells *in vivo*, the route of administration of pCSNPs must be systematically studied and optimized for immunotherapeutic applications. Further, a targeted gene delivery approach through suitable modification of the nanoparticles could also be explored as a future direction. Other conventionally available transfection agents, such as cell-penetrating peptides (CPPs), PF14, or PEI, when complexed with plasmids have limitations, such as instability, rapid opsonization, and toxicity [11]. In contrast, the CSNPs developed in this study were found to be safe with no *in vivo* toxicity, demonstrating their promise as non-viral gene delivery vehicles.

4. Conclusion

In this study, ionotropic gelation technique was used to form chitosan polyplexes with structural stability and ability to encapsulate, protect and deliver pDNA. Our results show that several factors need to be considered in order to design these gene delivery vehicles to achieve homogeneity of the NPs and prevent their aggregation, which could interfere with cellular uptake. Among various conditions and parameters, the concentration and volume of chitosan (CS) and tripolyphosphate (TPP) were most critical in controlling the size, stability, encapsulation efficiency, surface charge, and morphology of the NPs. In this work, the effectiveness of pCSNP for *in vitro* transfection in immune cells and *in vivo* transfection has been demonstrated. Their potential to boost gene expression in target immune cells makes them an ideal platform for immunotherapeutic applications such as cancer and autoimmune diseases. The use of chitosan nanoparticles presents a biocompatible, non-viral, and potentially safer approach to gene delivery. This study can further be extended to targeted delivery of nanoparticles through surface modification of CSNPs with appropriate ligands for organ specific immunotherapeutic applications, and opening up newer frontiers in gene therapy.

Acknowledgements

The authors would like to express their gratitude to the National Technical Textile Mission (NTTM, Ministry of Textiles, India) for providing the funding necessary to conduct this study. We also wish to acknowledge Mr. Vishal Mourya, Project Technical Assistant, for his invaluable help with animal experiments and IVIS image analysis.

Authors' contribution

Conceptualization and planning of experiments, synthesis and characterization of the nanoparticles, *in vivo* studies, data analysis, and writing—original draft preparation, MMP; *in vitro* transfection, flow cytometry analysis, and writing—review and editing, HD; cytocompatibility, *in vivo* biocompatibility studies, flow cytometry analysis, writing—original draft preparation, and writing—review and editing, MS; isolation and characterization of plasmids, AS; conceptualization and planning of experiments, supervision, project administration, funding acquisition, and writing—review and editing, PT. All authors have read and agreed to the published version of the manuscript.

Conflicts of interests

The authors declare no conflict of interest.

Ethical statement

In vivo experiments were conducted at the Laboratory Animal Facility, Advanced Centre for Treatment, Research and Education in Cancer (ACTREC), Mumbai as per the protocols approved by the Institute Animal Ethics Committee (IAEC 01/2022).

References

[1] Ashfaq M, Ahmad A. Chitosan and its derivatives-based dimensional frameworks as carrier for gene delivery. In *Polysaccharide-Based Nanocomposites for Gene Delivery and Tissue Engineering*, 1st ed. Amsterdam: Elsevier, 2021. pp. 41–57.

[2] Calvo P, Remuñan-López C, Vila-Jato JL, Alonso MJ. Chitosan and chitosan/ethylene oxide-propylene oxide block copolymer nanoparticles as novel carriers for proteins and vaccines. *Pharm. Res.* 1997, 14(10):1431–1436.

[3] Lara-Velazquez M, Alkharboosh R, Norton ES, Ramirez-Loera Cristopher, Freeman WD, *et al*. Chitosan-based non-viral gene and drug delivery systems for brain cancer. *Front. Neurol.* 2020, 11:740.

[4] Boussif O, Lezoualc'h F, Zanta MA, Mergny MD, Scherman D, *et al*. A versatile vector for gene and oligonucleotide transfer into cells in culture and in vivo: polyethylenimine. *Proc. Natl. Acad. Sci. U.S.A.* 1995, 92(16):7297–7301.

[5] Kurrikoff K, Veiman KL, Künnapuu K, Peets EM, Lehto T, *et al*. Effective *in vivo* gene delivery with reduced toxicity, achieved by charge and fatty acid-modified cell penetrating peptide. *Sci. Rep.* 2017, 7:17056.

[6] Aibani N, Rai R, Patel P, Cuddihy G, Wasan EK. Chitosan nanoparticles at the biological interface: implications for drug delivery. *Pharmaceutics* 2021, 13(10):1686.

[7] Aranda-Barradas ME, Coronado-Contreras HE, Aguilar-Castañeda YL, Olivo-Escalante KD, González-Díaz FR, *et al*. Effect of different karyophilic peptides on physical characteristics and *in vitro* transfection efficiency of chitosan-plasmid nanoparticles as nonviral gene delivery systems. *Mol. Biotechnol.* 2025, 67(2):723–733.

[8] Khan IN, Navaid S, Waqar W, Hussein D, Ullah N, *et al*. Chitosan-based polymeric nanoparticles as an efficient gene delivery system to cross blood-brain barrier: *in vitro* and *in vivo* evaluations. *Pharmaceuticals* 2024, 17(2):169.

[9] Antoniou V, Mourelatou EA, Galatou E, Avgoustakis K, Hatziantoniou S. Gene therapy with chitosan nanoparticles: modern formulation strategies for enhancing cancer cell transfection. *Pharmaceutics* 2024, 16(7):868.

[10] Corsi K, Chellat F, Yahia LH, Fernandes JC. Mesenchymal stem cells, MG63 and HEK293 transfection using chitosan—DNA nanoparticles. *Biomaterials* 2003, 24(7):1255–1264.

[11] Zhang K, Fang H, Chen Z, Taylor JSA, Wooley KL. Shape effects of nanoparticles conjugated with cell-penetrating peptides (HIV Tat PTD) on CHO cell uptake. *Bioconjugate Chem.* 2008, 19(9):1880–1887.

[12] Lee J, Yun KS, Choi CS, Shin SH, Ban HS, *et al*. T cell-specific siRNA delivery using antibody-conjugated chitosan nanoparticles. *Bioconjugate Chem.* 2012, 23(6):1174–1180.

[13] Huang Y, Lapitsky Y. Salt-assisted mechanistic analysis of chitosan/tripolyphosphate micro- and nanogel formation. *Biomacromolecules* 2012, 13(11):3868–3876.

[14] Alswailem R, Alqahtani FY, Aleanizy FS, Alrfaei BM, Badran M, *et al*. MicroRNA-219 loaded chitosan nanoparticles for treatment of glioblastoma. *Artif. Cells Nanomed. Biotechnol.* 2022, 50(1):198–207.

[15] Abdul Ghafoor Raja M, Katas H, Jing Wen T. Stability, intracellular delivery, and release of siRNA from chitosan nanoparticles using different cross-linkers. *PLoS One* 2015, 10(6):e0128963.

[16] Chithrani BD, Ghazani AA, Chan WCW. Determining the size and shape dependence of gold nanoparticle uptake into mammalian cells. *Nano Lett.* 2006, 6(4):662–668.

[17] Karimi M, Avci P, Ahi M, Gazori T, Hamblin MR, *et al*. Evaluation of chitosan-tripolyphosphate nanoparticles as a p-shRNA delivery vector: formulation, optimization and cellular uptake study. *J. Nanopharm. Drug Delivery* 2013, 1(3):266–278.

[18] Foroozandeh P, Aziz AA. Insight into cellular uptake and intracellular trafficking of nanoparticles. *Nanoscale Res. Lett.* 2018, 13:339.

[19] Rahimmanesh I, Totonchi M, Khanahmad H. The challenging nature of primary T lymphocytes for transfection: effect of protamine sulfate on the transfection efficiency of chemical transfection reagents. *Res. Pharm. Sci.* 2020, 15(5):437.

[20] Sabin J, Alatorre-Meda M, Miñones J, Domínguez-Arca V, Prieto G. New insights on the mechanism of polyethylenimine transfection and their implications on gene therapy and DNA vaccines. *Colloids Surf. B Biointerfaces* 2022, 210:112219.

[21] Malatesta M, Grecchi S, Chiesa E, Cisterna B, Costanzo M, *et al*. Internalized chitosan nanoparticles persist for long time in cultured cells. *Eur. J. Histochem.* 2015, 59(1):2492.

[22] Raftery R, O'Brien FJ, Cryan SA. Chitosan for gene delivery and orthopedic tissue engineering applications. *Molecules* 2013, 18(5):5611–5647.